

# Including in-vivo IVUS data in ex-vivo validated dataset

Francesco Ciompi\*, Oriol Pujol<sup>+</sup> and Petia Radeva\*

\* *Computer Vision Center, Universitat Autnoma de Barcelona*  
E-mail: f.ciompi@cvc.uab.es - petia@cvc.uab.es

<sup>+</sup> *Departament de Matemàtica Aplicada i Anlisi, Universitat de Barcelona*  
E-mail: oriol@maia.ub.es

**Abstract** Intravascular Ultrasound (IVUS) data validation is usually performed by comparing post-mortem (*ex-vivo*) IVUS data and corresponding histological analysis of the tissue, obtaining a reliable *ground truth*. The main drawback of this method is the few amount of available training dataset. In this work we propose a method to include examples from *in-vivo* labeled plaque to the *ex-vivo* training dataset. *In-vivo* plaques selection is performed by Sequential Floating Forward Selection (SFFS) algorithm and results are validated by the Leave-One-Patient-Out cross-validation technique. Classification task is performed by using *AdaBoost* exploiting the *Error Correcting Output Code* (ECOC) technique to infer the final decision. New data inclusion improves global classification accuracy from 89.56% to 91.77%.

## 1 Introduction

Coronary plaque rupture is one of the most frequent case of acute coronary syndromes and it can end in myocardial infarction or sudden cardiac death [2] [6] [?]. An accurate *in-vivo* plaque composition identification represents an important task in diagnosis and detection of vulnerable atheroma before plaque rupture. IVUS is a powerful imaging technique that gives a detailed cross-sectional image of the vessel allowing to explore both coronary arteries morphology and composition.

Plaque composition can be determined by texture analysis on IVUS images [13] [15] as well as performing a spectral analysis on the original Raw Radio Frequency (RF) signals [11] [9] [10] [4].

During an IVUS analysis, physicians typically change IVUS imaging parameters making the study from different cases and consequently extracted fea-

tures non comparable. An IVUS images reconstruction process from RF signals can avoid this kind of problems, adopting a unique well defined parameters set. Finally, both textural and spectral features can be extracted to train a classifier for automatic plaque characterization process. In this work we want to discriminate among *fibrotic*, *lipidic* and *calcified* tissue.

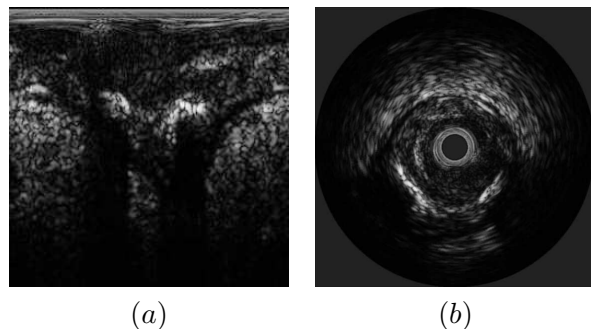


Figure 1: (a) IVUS image in polar coordinates; (b) IVUS image in cartesian coordinates

In order to validate IVUS data, typical adopted technique consists in analyzing *post-mortem* (*ex-vivo*) coronary arteries by histological analysis. The main problems of this protocol are few data availability because of scarce artery availability, tissue spoiling during histological analysis, frequent mismatching between IVUS and histological image and finally a long time needed from data acquisition to final histological results. As counterpart, provided data are highly reliable.

On the contrary, *in-vivo* data collection is an easy task but obtained information cannot be validated.

We propose here a method to select *in-vivo* plaques to feed the training *ex-vivo* dataset with data that improve classifier performances. The inclusion criterion is based on *Selection Fast Forward Search*

(SFFS) algorithm by maximizing at each search step the weighted sensitivity for each class. Classification performance is validated by *Leave-One-Patient-Out* (LOPO) cross-validation technique.

The multiclass classification problem is here solved by adopting the powerful *Error Correcting Output Code* (ECOC) technique [5] [1] using Adaboost as basic classifier.

## 2 IVUS data processing

An IVUS study consists in introducing a catheter carrying an ultrasound transducer inside the coronary artery through the femoral or radial vessels. The IVUS equipment used in this work is a *Galaxy 2 IVUS Imaging System* (Boston Scientific) with a catheter *Atlantis SR Pro 40 MHz* (Boston Scientific). RF data are collected by a *12-bit Acquiris acquisition card* with a sampling rate of *200 MHz*. Each RF data frame is stored in a matrix of 1024 samples and 256 A-lines.

**Image reconstruction** RF data are processed to reconstruct IVUS images and to extract textural and spectral features. First, a *Time Gain Compensation* is applied, to compensate the US attenuation due to reached depth, then each signal is filtered *Band Pass* around the catheter central frequency ( $f_0 = 40\text{MHz}$ ) to attenuate noise contribution. The *envelope* of each signal is then recovered by the Hilbert transform. After *normalizing* the signal range between 0 and 1, *logarithmic compression* is applied in order to enhance low grey level visualization and finally a *gamma correction* expands image dynamic. Final step is a *Digital Development Process* that consists in radial contrast tuning and edge emphasis phenomenon.

Standard IVUS image is produced by converting obtained data in Cartesian coordinates. Linear interpolation and Gaussian smooth filtering are used.

**Power Spectrum Computation** RF signals power spectrum can be computed by using *AutoRegressive Models* (ARM), one of the most suitable and stable methods to analyze ultrasound signals [11].

ARM are defined as a linear prediction equation where the output  $x$  at a certain point  $t$  for each A-line is equal to a linear combination of its  $p$  previous

outputs weighted by a set of parameters  $a_p$  [12]:

$$x(t) = \sum_{k=1}^p a_p(k)x(t-k) \quad (1)$$

where  $p$  is the ARM degree and the coefficients  $a_p$  are calculated minimizing the error of the modelled spectrum with respect to original one using the Akaike's error prediction criterion [12]. As in [11] in this work we used  $p = 10$ . A sliding window is formed by  $n$  samples and  $m$  contiguous A-lines with a displacement of  $n/4$  samples and  $m/3$  A-lines in order to obtain an averaged AR model of a region. Only one side of the obtained spectrum is used because of its symmetrical properties. Used values are  $n = 64$  and  $m = 12$ .

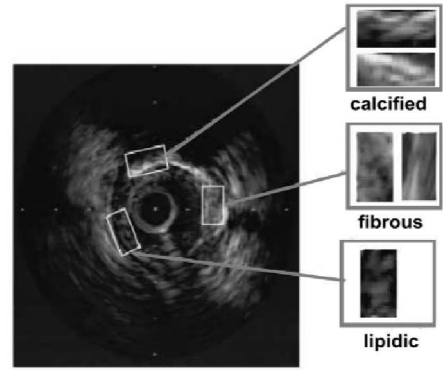


Figure 2: Different plaque types in IVUS image

## 3 Features Extraction

**Image features** Textural features are extracted by using the following texture descriptors: Gabor filters, Local binary patterns, the mean value and the shading of the polar image.

A *Gabor filter* is a special case of wavelets which is essentially a Gaussian modulated by a complex sinusoid. In this work we used a bank of 16 filters obtained by varying the gaussian standard deviation  $\sigma$  and the 2D frequencies  $(F, \phi)$  of the complex sinusoid, expressed in polar form. Used values are:  $\sigma = [12.7205, 6.3602, 3.1801, 1.5901]$  and  $(F, \phi) = [(0.0442, 0^\circ) (0.0884, 45^\circ) (0.1768, 90^\circ) (0.3536, 135^\circ)]$ .

*Local Binary Patterns* (LBP) are used to detect uniform texture patterns in circular neighbourhoods

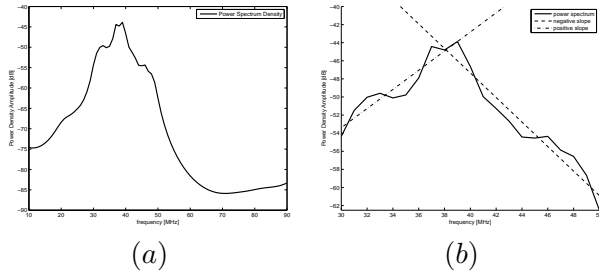


Figure 3: (a) Typical Power Density Spectrum profile; (b) Straight lines for slopes computation

with any quantization of angular space and spatial resolution [3]. LBP are based on a circular symmetric neighborhood of  $P$  members with radius  $R$ . To achieve gray level invariance, the central pixel  $g_c$  is subtracted to each neighbor  $g_p$ , assigning the value 1 to the result if the difference is positive and 0 otherwise:  $LBP_{R,P} = \sum_{p=1}^P a(g_p - g_c) \cdot 2^p$ . We used radius of  $R = [1, 2, 3]$  pixels and corresponding neighbourhoods of  $P = [8, 16, 24]$  pixels.

The mean grey level value is computed for each point using a window of  $12 \times 12$  pixel. The inclusion of this feature takes sense as different plaque types typically show different gray level intensity.

As highlighted in [7], *calcified* plaque, due to its natural low echo reflectance property, appears as a bright area followed by a black area, that we call *shadow* and that can be detected by accumulating the grey level value starting from the external part of each radius towards the center:  $S(x, y) = \sum_{y^*=y}^{r_{MAX}} I(x, y^*)$ , where  $I(x, y)$  is the IVUS image in polar coordinates and  $r_{MAX}$  is the maximum radial depth.

**Spectral features** From each point of the IVUS image we compute a power spectrum, as explained in section 2. The central frequency of the catheter is  $f_0 = 40 MHz$  and a typical Power Spectral Density (PSD) profile is illustrated in Figure 3(a). We limit spectral information to a band  $B = f_H - f_L$  ( $f_L = 30 MHz$ ,  $f_H = 50 MHz$ ). Given spectral content in a band  $30 MHz \leq B \leq 50 MHz$  and defining  $f_{max} : S(f_{max}) = \max(S(f)|_{f \in B})$ , we consider two curves:  $S_+ = S(f_L \div f_{max})$ ,  $S_- = S(f_{max} \div f_H)$ . Now it is possible to compute the lines  $l_+$  and  $l_-$  that linearly fit the two curves. From these lines we can extract *positive slope*, *negative*

*slope*, *positive y-intercept* and *negative y-intercept* features (Figure 3(b)). Then we can compute the *mean power* as  $\frac{1}{B} \sum_{f=f_L}^{f=f_H} S(f)$ , the *maximum power in B* as  $\max(S(f))$ , the *power at  $f_L$*  as  $S(f_L)$ , the *power at  $f_H$*  as  $S(f_H)$  and the *power at  $f_0$*  as  $S(f_0)$ .

In addition, two global measures are computed: the *energy of A-line* and the *energy of the window spectrum*. As described in previous sections, shadow is an important feature in *calcified* tissue detection. Two values related to shadow are then computed using raw RF data as well.

The final feature vector is formed by the union of both textural and spectral features, since this combination showed improvements in classification task [3].

## 4 Classification

Once we reconstructed image, computed power spectrum and extracted features, a classification scheme is developed. Since we want to discriminate among *fibrotic*, *lipidic* and *calcified* tissue, a multiclass problem arises.

Error Correcting Output Code is a novel technique that allows to reduce *multiclass* classification problem to a set of *binary* classification problems [1] [5]. Given a certain number of  $N$  classifiers (dichotomies)  $h_i$  ( $i = 1, \dots, N$ ), for each one of the  $K$  classes, a particular *codeword*  $c_j$  ( $j = 1, \dots, K$ ) of values  $\{1, 0, -1\}$  with a length equal to the classifiers number is created, obtaining the so-called ECOC matrix: each column represents a binary classifier (dichotomy), each row represents a class. A value 1 in position  $m_{kh}$  means that the classifier  $h$  classifies the point as belonging to the class  $k$ , a value -1 means that the point belongs to the class  $q \neq k$  and a 0 value means that we do not care about the result of classifier  $h$ , considering class  $k$ . Given the codeword obtained by applying the whole classifiers set over an example, the distance between the codeword and each row  $m_j$  is computed: the final inference about a class will be the value  $j$  corresponding to the minimum distance between the given codeword and each row of the  $M$  matrix. In this work we used the *Euclidean* distance. Used ECOC matrix  $M$  in our three classes problem, adopting *1vs1* technique is the following:

$$\mathbf{M} = \begin{pmatrix} 1 & 1 & 0 \\ -1 & 0 & 1 \\ 0 & -1 & -1 \end{pmatrix}$$

The classifier used in this work to build dichotomies is *AdaBoost* [8] [14]. It calls a weak classifier  $h_t$  repeatedly in a series of rounds  $t = 1, \dots, T$ : for each call a distribution of weights  $D_t$  is updated that indicates the importance of examples in the data set for the classification. On each round, the weights of each incorrectly (correctly) classified example are increased (decreased), so that the new classifier focuses more on those examples. The weak learner used in this work is *decision stumps*. Convergence is reached by using  $T = 50$ .

## 5 In-vivo IVUS data

*In-vivo* data extraction is performed during a normal surgery operation. As the catheter is connected to the IVUS equipment by a motorized tool, when the surgery is over, it is possible to acquire an *IVUS Pull-back*: we just need to perform data acquisition while the probe is *pulled-back* at constant speed.

The main advantage of *in-vivo* analysis is the acquisition of a large amount of images for each patient and the possibility to perform it during each surgery operation. The drawback is that acquired data cannot be validated. Given a set of *in-vivo* images, in fact, expert physicians can manually segment plaques, labeling them according only on their opinion given by their professional experience. In order to obtain more reliable segmentation we can let more than one physicians to segment plaques and then to extract features only from common regions.

Given the large and relatively easy availability of *in-vivo* data, our goal is to find a way to include these data into the *ex-vivo* validated training set, in order to improve classification performance. As the obtained data set cannot be used as *ground truth*, our problem can be viewed as a *semi-supervised learning* problem [17]. We have in fact an *ex-vivo* validated data *ground truth* and a set of unreliable labeled data to include into the training set. Our hypothesis is that this selected additional data set carries point with the same spatial distribution, for each class, of the validated training set. *In-vivo* plaques selection is

performed by *Sequential Floating Forward Selection* (SFFS) [16].

## 6 Methodology

Performances of classifiers are evaluated by *cross validation*, using a part of the whole data set as *training* and the remaining as *test*. The cross-validation technique used here is the *Leave-One-Patient-Out*.

**Leave One Patient out** Let us call  $N_p$  the number of cases. Our training data come from *ex-vivo* (*necro*) analysis and we have a certain number of images for each case, depending on the lesions quantity. The training set is built taking all data for each case (a set of images from the same *necro* case) except one case, used as test. The process is repeated for each patient and confusion matrix is computed at each round. Parameters are computed as:  $A_{LOPO} = \frac{1}{N_p} \sum_{i=1}^{N_p} A(i)$ ,  $S_{LOPO}^l = \frac{1}{N_p} \sum_{i=1}^{N_p} S^l(i)$ , where  $A = \frac{\sum_{i=1}^{N_c} c_{ii}}{\sum_{i=1}^{N_c} \sum_{j=1}^{N_c} c_{ij}}$  is the global accuracy and  $S^l = \frac{c_{ll}}{\sum_{i=1}^N c_{li}}$  is the sensitivity for each class;  $N_c$  is the classes number,  $c$  is an element of the confusion matrix  $C$  and  $l$  indicates a particular class.

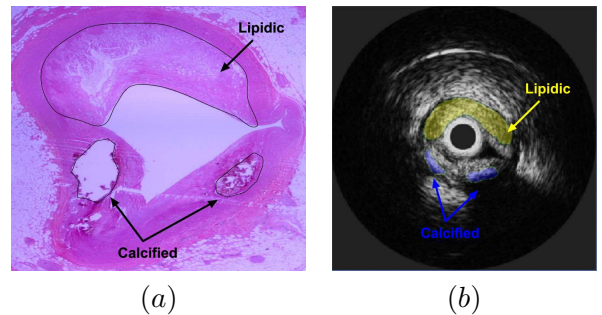


Figure 4: (a) Histological image and (b) corresponding IVUS image

**In-vivo data selection** Let us call  $x$  the *in-vivo* plaques set in a single frame extracted from an *in-vivo* case, initially belonging to the set  $Y$ ,  $X$  the final training set, initially composed only by *ex-vivo* data,  $k$  the algorithm iteration. Let us also define  $J$  as the parameter related to the classification performance. Used criterion assumes  $J$  as the weighted sensitivity, in order to avoid a global parameter improving by increasing classification performances in

one or more class while decreasing the remaining. Each weight is considered as inversely proportional, according to a logarithmic law, to the sensitivity of each class computed at the actual algorithm step  $k$ . Finally, the parameter computed at each step is  $J_k = \sum_{l=1}^{N_c} w_l \cdot S_k^l$ , where  $w_l = \log(\frac{1}{S_k^l}) / \sum_{l=1}^{N_c} \log(\frac{1}{S_k^l})$ .

---



---

#### SFFS ALGORITHM

---



---

*Input:*  $Y = \{y_j \mid j = 1, \dots, D\}$

*Output:*  $X_k = \{x_i \mid j = 1, \dots, k, x_j \in Y\}, k = 0, 1, \dots, D$

*Initialization:*  $X_0 = 0, k = 0$

Stop when  $k$  equals the number of plaques required

##### STEP 1

*Inclusion:*  $x^+ = \arg \max_{x \in Y - X_k} \{J(X_k + x)\}$ ;

$X_{k+1} = X_k + x^+; k = k + 1$

##### STEP 2

*Conditional Exclusion:*  $x^- = \arg \max_{x \in X_k} J(X_k - x)$

if  $J(X_k - x^-) > J(X_{k-1})$

then

$X_{k-1} = X_k - x^-; k = k - 1$ ; goto STEP 2

else

goto STEP 1

$X_{k+1} = X_k + x^+; k = k + 1$

---



---

## 7 Results

Ex-vivo data have been extracted from 9 *ex-vivo* cases with 26 *fibrotic*, 14 *lipidic* and 31 *calcified* plaques. Data have been validated by histological analysis. *In-vivo* data are taken from 9 patients, plaques are labeled by two expert physicians collecting 49 *fibrotic*, 37 *lipidic* and 35 *calcified* plaques. Ex-vivo data classification task, using AdaBoost and ECOC technique has been validated by LOPO cross-validation in terms of sensitivity for each class and global accuracy.

In-vivo data inclusion by SFFS selection has been repeated varying the percentage of included *in-vivo* data from 10% to 50%. Including more than 50% reduces too much the role of the validated training set. Since the examples are taken by downsampling in number the whole data set, in order to obtain robust results, we repeated the process 10 times, averaging final results.

The best percentage of *in-vivo* data results to be 30%. The algorithm finds continuous improvement

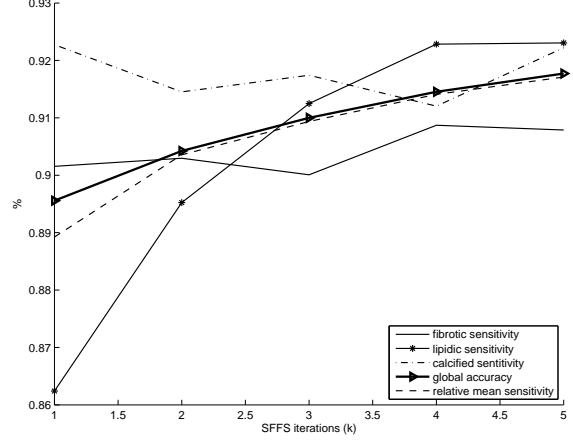


Figure 5: SFFS results

by selecting 4 *in-vivo* frames from 3 cases, collecting 1 *fibrotic*, 2 *lipidic* and 2 *calcified* plaques. Improvements in terms of sensitivity and global accuracy are explained in following table:

	before inclusion	after inclusion
$S_{LOPO}^{fib}$	90.15% ± 9.34	<b>90.79% ± 9.66</b>
$S_{LOPO}^{lip}$	86.24% ± 12.88	<b>92.30% ± 7.29</b>
$S_{LOPO}^{cal}$	92.27% ± 4.32	<b>92.22% ± 5.93</b>
$A_{LOPO}$	89.56% ± 7.53	<b>91.77% ± 6.53</b>

## 8 Conclusions and future works

A framework for IVUS image reconstruction and power spectrum computation from raw radio frequency data extracted and validated from ex-vivo cases has been presented as well as both textural and spectral features extraction process for robust tissue characterization.

*In-vivo* data acquisition process has been described and feature extraction has been performed. It has been demonstrated that the inclusion of selected *in-vivo* data in the *ex-vivo* training set improves both individual sensitivities and overall accuracy. As illustrated in Figure 5, *lipidic* class obtains the most benefit in term of improvement. This is explicable by considering that in the original *ex-vivo* training set the number of *lipidic* plaque is much less than the other. Then, given the relatively low initial sensitivity in *lipidic* classification, our algorithm goes for improvement in terms of *lipidic* sensitivity.

Here we showed that the inclusion of *in-vivo* data

improves classification performances by using AdaBoost. A deeper study using the combination of several classifiers in the *in-vivo* selection process can be performed. The main drawback of this method is the large time needed to converge. Moreover, in the case here analysed, the algorithm stop at iteration 5 (Figure 5). This happens since given the available *in-vivo* plaques set, further addition decrease global accuracy in next step. Another way to exploit *in-vivo* inclusion could be to study its behaviour in including a large number of plaques, accepting for temporary accuracy reduction.

Finally, *in-vivo* data are here included by using SFFS algorithm that is simply a selection algorithm. Our purpose is to study more *semi-supervised* techniques and to use other multiclass classifiers to achieve a better separation between *ex-vivo* and *in-vivo* data and a more precise selection.

## References

- [1] E. L. Allwein et al., "Reducing multiclass to binary: A unifying approach for margin classifiers" *Journal of Machine Learning Research*, 1: 113–141, 2000.
- [2] A. P. Burke et al. "Coronary risk factors and plaque morphology in men with coronary disease who died suddenly". *The New England Journal of Medicine*, 336(18):1276–1282, 1997.
- [3] K. L. Caballero. "Coronary Plaque Classification Using Intravascular Ultrasound Images and Radio Frequency Signals" Universitat Autònoma de Barcelona, 2007.
- [4] A. N. DeMaria et al. "Imaging vulnerable plaque by ultrasound" *Journal of the American College of Cardiology*, 47(8):C32–9, 2006.
- [5] T. G. Dietterich and G. Bakiri. "Solving multi-class learning problems via error-correcting output codes" *Journal of Artificial Intelligence Research*, 2:263–286, 1995.
- [6] S. Ehara et al. "Spotty calcification typifies the culprit plaque in patients with acute myocardial infarction: An intravascular ultrasound study" *Circulation*, 110:3424–3429, 2004.
- [7] E. D. Filho et al. "A study on intravascular ultrasound image processing, 2005"
- [8] J. Friedman, T. Hastie, and R. Tibshirani. "Additive logistic regression: a statistical view of boosting" *Annals of Statistics*, 28:2000, 2000.
- [9] M. P. Moore et al. "Characterization of coronary atherosclerotic morphology by spectral analysis of radiofrequency signal: in vitro intravascular ultrasound study with histological and radiological validation". *Heart*, 79:459–467, 1998.
- [10] A. Murashige et al. "Detection of lipid-laden atherosclerotic plaque by wavelet analysis of radiofrequency intravascular ultrasound signals". *Journal of the American College of Cardiology*, 45(12):1954–1960, 2005.
- [11] A. Nair et al. "Coronary plaque classification with intravascular ultrasound radiofrequency data analysis". *Circulation*, 106:2200–2206, 2002.
- [12] J. Proakis, C. Rader, F. Ling, and C. Nikias. "Advanced Digital Signal Processing". Mc.Millan, 1992.
- [13] O. Pujol. "A Semi-Supervised Statistical Framework and Generative Snakes for IVUS Analysis". Universitat Autònoma de Barcelona, 2004.
- [14] R. E. Schapire. "The boosting approach to machine learning: An overview", 2002.
- [15] X. Zhang, C. R. McKay, and M. Sonka. "Tissue characterization in intravascular ultrasound images". *IEEE Transaction on Medical Imaging*, 17(6):889–899, 1998.
- [16] P. Pudil, F. J. Ferri and J. Kittler. "Floating search methods for feature selection with non-monotonic criterion functions", *IAPR* 279–283, 1994.
- [17] X. Zhu. Semi-supervised learning literature survey, 2008.